Air-Pressure Servoing for Robotic Grasping with Multi-Cup Suction Grippers

Alejandro Velasquez[1], Olivia Gehrke[1], Cindy Grimm[1], Joseph R. Davidson[1]

***Abstract*—In selective fruit harvesting, the localization of the fruit is prone to noise and sensor inaccuracy. These inaccuracies lead to inappropriate misalignment between the end effector and the fruit which hinders grasp and pick operations. Computer vision and depth perception techniques are able to locate the fruit with relatively good precision; however, these sensors work up to a certain proximity to the fruit where other near-contact perception and actuation should be used. We use a multi-cup suction gripper endowed with air-pressure sensors to account for the engagement of each suction cup. Moreover, we map the addition of the air-pressure vectors into an axis-angle rotation representation and servo the gripper until all suction cups engage. Furthermore, we locate the center of rotation near the engaged suction cup(s) to reduce the slippage and tangential forces between the suction cups and the fruit. We attach our gripper to a UR5e manipulator and perform apple pick trials using an apple proxy. We vary the branch stiffness and offset the location of the gripper w.r.t. fruit by $10mm$, $20mm$, and $30mm$, and measure the elapsed time until all suction cups engage. We observe that elapsed time increases when the branch has low stiffness and with the offset. In all the cases, the gripper engaged all suction cups and successfully picked the fruit.**

I. Introduction

In recent years, robotic apple picking has become a very active area of research with much of the focus being on the best features of an End Effector (EEF). One of the main issues with robotic harvesting is that the EEF is often misaligned with the fruit [1], [2]. This can be due to sensor noise, occlusions, or differing apple shapes [3]. While various forms of visualization have been used to center an apple within an EEF's grasp, occlusion and sensor noise have caused these methods to be unreliable [1]. These interferences can hinder the EEF's actuation means from fully engaging with the fruit, which can decrease the success rate of apple picking [1].

Perception techniques such as visual and depth-based work up to a certain proximity with the target. However, other techniques such as tactile perception should be used for near-contact distances. Quasi tactile perception can be achieved using suction cups, by adding air-pressure sensors near the vacuum chambers. Different approaches have been used for picking up objects with suction cups. Lee et al. proposed utilizing multiple suction cups arranged in a pattern to pick up objects [4]. In another work, the author used a suction cup with four chambers with the positioning controlled by pressure differentials [5]. One difference with our application is that in both works, the objects being picked were supported by a surface. In contrast, in selective fruit harvesting, fruit are hanging from a stem, and may swing away when pushed by the EEF. Moreover, while manipulating a single suction cup is helpful for smaller objects, having a singular suction cup isn't enough to center and stabilize an apple for a pick to occur.

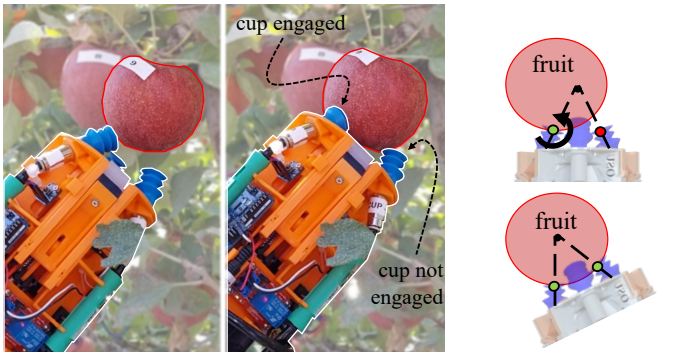

Initial cup engagement — Gripper pose adjustment

Fig. 1: *Left*: Sequence of an apple pick with our multi-cup suction gripper [1]. Notice that one suction cup did not engage. *Right*: Pose adjustment by rotating the gripper w.r.t. engaged suction cups (shaded green) until the remaining cups engage.

In this work, we use a multi-cup suction gripper endowed with three suction cups and air pressure sensors [1]. We adjust the angular orientation of the EEF by air-pressure servoing to engage all the suction cups with the fruit. We use air-pressure vector addition to obtain a net air-pressure vector and map it into the axis and angle of rotation. Moreover, we locate the center of rotation near the suction cup(s) engaged to reduce tangential forces and slippage between the suction cups and the fruit. This air-pressure servoing results in centering the EEF with respect to the fruit within in-contact distances where other perception techniques are not feasible (e.g. vision, radar). We test the performance using an apple proxy [2], and vary the fruit dynamics stiffness. Furthermore, we mimic sensor noise by intentionally adding an offset location of the gripper w.r.t. apple ($10mm$, $20mm$, and $30mm$).

II. Methodology

We use air-pressure vectors associated with each suction cup for servoing the orientation of the EEF. We use vector addition to find the net air-pressure vector, and use it to obtain the angle and axis of rotation. Moreover, we locate the center of rotation near the suction cups engaged to minimize slippage between the suction cups and the fruit surface.

This research is supported by the United States Department of Agriculture (USDA)-National Institute of Food and Agriculture (NIFA) through the Cyber Physical Systems program (Award No. 2020-67021-31525).

[1]Collaborative Robotics and Intelligent Systems (CoRIS) Institute, Oregon State University, Corvallis, OR 97331, USA. {velasale, gehrkeo, grimmc, joseph.davidson}@oregonstate.edu

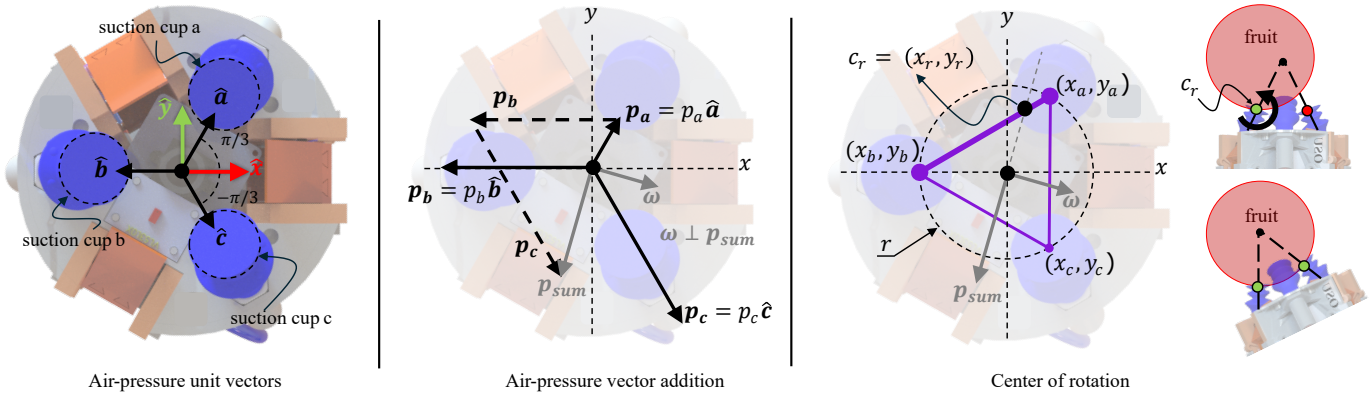

Fig. 2: Mapping air-pressure readings into EEF vector mechanics. *Left*: Gripper top view with three suction cups and their respective air-pressure unit vectors. *Middle*: Vector addition of air-pressure readings to obtain net vector p_{sum}. The angle of rotation θ is proportional to the magnitude of p_{sum}, and the axis of rotation ω is orthogonal to p_{sum}. In this example, suction cup a is highly engaged, suction cup b is somewhat engaged, and suction cup c is disengaged. *Right*: Location of center of rotation c_r. When two suction cups are engaged with the fruit, c_r is located at the intersection between vector p_{sum} and the line between the engaged suction cups. If only one suction cup is engaged, c_r is located at the center of that suction cup.

A. Air-pressure readings

We use a multi-cup suction gripper from our previous work [1]. Our gripper uses three decentralized vacuum ejectors (PIAB PiINLINE Micro Ti, 6-6mm) connected to each of the three suction cups (PIAB F-BX20) and air-pressure sensor (Adafruit MPRLS). The sensors' readings range between the atmospheric pressure (when suction cups are disengaged) and $\sim$ 80% of vacuum (when suction cups are engaged). At sea level, these values range between $\sim$ 100 kPa (when disengaged) and $\sim$ 20 kPa (when engaged). Note that vacuum is inverse to air-pressure readings.

B. Transformation matrix

We map the air-pressure readings into an axis-angle representation and elaborate the rotation matrix. Then, we locate the center of rotation c_r at the suction cup(s) with the highest vacuum, which defines the translation vector from the center of the . Finally, we elaborate the transformation matrix with the rotation matrix and the translation vector.

1) Axis of rotation ω: We associate an air-pressure vector for each suction-cup in a c-frame located at the center of the gripper. The orientation of each air-pressure unit vector is defined by the location of its respective suction cup as shown in fig. 2-*Left*. Moreover, the magnitude of each air-pressure vector is given by each air-pressure reading (p_a, p_b, and p_c). These vector definitions are expressed from eq. (1) to eq. (6)).

$$\mathbf{p_a} = p_a \cos\left(\frac{\pi}{3}\right)\hat{\mathbf{x}} + p_a \sin\left(\frac{\pi}{3}\right)\hat{\mathbf{y}} \tag{1}$$

$$\mathbf{p_a} = \frac{1}{2}p_a\hat{\mathbf{x}} + \frac{\sqrt{3}}{2}p_a\hat{\mathbf{y}} \tag{2}$$

$$\mathbf{p_b} = p_b \cos(\pi)\hat{\mathbf{x}} + p_b \sin(\pi)\hat{\mathbf{y}} \tag{3}$$

$$\mathbf{p_b} = -p_b\hat{\mathbf{x}} \tag{4}$$

$$\mathbf{p_c} = p_c \cos\left(-\frac{\pi}{3}\right)\hat{\mathbf{x}} + p_c \sin\left(-\frac{\pi}{3}\right)\hat{\mathbf{y}} \tag{5}$$

$$\mathbf{p_c} = \frac{1}{2}p_c\hat{\mathbf{x}} - \frac{\sqrt{3}}{2}p_c\hat{\mathbf{y}} \tag{6}$$

Next, by vector addition we obtain the net vector p_{sum} which serves twofold: (i) we use its orthogonal vector ω as the *axis of rotation*, and (ii) we use its magnitude to calculate the *angle of rotation*, as shown from eq. (7) to eq. (11).

$$\mathbf{p_{sum}} = \mathbf{p_a} + \mathbf{p_b} + \mathbf{p_c} \tag{7}$$

$$\mathbf{p_{sum}} = \left(\frac{1}{2}(p_a + p_c) - p_b\right)\hat{\mathbf{x}} + \frac{\sqrt{3}}{2}(p_a - p_c)\hat{\mathbf{y}} \tag{8}$$

$$\omega \perp \mathbf{p_{sum}} \tag{9}$$

$$\omega = \frac{\sqrt{3}}{2}(p_a - p_c)\hat{\mathbf{x}} + \left(\frac{1}{2}(p_a + p_c) - p_b\right)\hat{\mathbf{y}} \tag{10}$$

$$\hat{\omega} = \frac{\omega}{\|\omega\|} \tag{11}$$

2) Angle of rotation θ: . We assume the amount of rotation to be proportional to the norm of p_{sum}, and use a proportional position controller eq. (12).

$$\theta = K_p\|\mathbf{p_{sum}}\| \tag{12}$$

3) Rotation Matrix: . We build the rotation matrix by using Rodrigues' formula [6] and the rotation axis and angle from eq. (11) and eq. (12):

$$\text{Rot}(\hat{\omega}, \theta) = e^{[\hat{\omega}]\theta} = I + \sin\theta\,[\hat{\omega}] + (1 - \cos\theta)\,[\hat{\omega}]^2 \tag{13}$$

4) Center of Rotation: . Suction cups dislike shear forces, and may wrinkle when subject to tangential forces. Hence, we place the center of rotation c_r at the center of the suction cup(s) engaged, depending on whether just one or two suction cups engaged. When just one suction is engaged, we place c_r at the center of that suction cup. On the other hand, when two suction cups engage, we locate c_r at the intersection between the net vector p_{sum} and the line between the engaged suction cups, as shown in fig. 2-*Right*. In our gripper, the suction cups are uniformly distributed around a circle with radius r. We use the coordinates of the center of each suction cup (Eqn. 14 to 16) to define the line equations $\bar{ab}$, $\bar{bc}$, and $\bar{ac}$ (Eqn. 17 and 18). Moreover, we use eq. (8) to obtain the equation of the line aligned with vector p_{sum} (19).

$$(x_a, y_a) = \left(\frac{1}{2}r, \frac{\sqrt{3}}{2}r\right) \tag{14}$$

$$(x_b, y_b) = (-r, 0) \tag{15}$$

$$(x_c, y_c) = \left(\frac{1}{2}r, \frac{-\sqrt{3}}{2}r\right) \tag{16}$$

$$y = \begin{cases} \frac{\sqrt{3}}{3}(x+r), & \text{if } p_a, p_b < p_{\text{atm}} \\ -\frac{\sqrt{3}}{3}(x+r), & \text{if } p_b, p_c < p_{\text{atm}} \end{cases} \tag{17}$$

$$x = \frac{1}{2}r, \quad \text{if } p_a, p_c < p_{\text{atm}} \tag{18}$$

$$y = \frac{\sqrt{3}(p_a - p_c)}{p_a + p_c - 2p_b}\, x \tag{19}$$

Next, we solve the system of equations (from eq. (17) to eq. (19)) to obtain the center of rotation c_r for each suction cup pair (ab, bc, and ac). Solutions for cases $\bar{ab}$, $\bar{bc}$, and $\bar{ac}$ are shown in eq. (20), eq. (21), and eq. (22) respectively.

$$c_{r(\bar{ab})} = \frac{r}{2}\begin{bmatrix} \frac{p_a+p_c-2p_b}{p_a-2p_c+p_b} & \frac{\sqrt{3}(p_a-p_c)}{p_a-2p_c+p_b} & 0 \end{bmatrix}^T \tag{20}$$

$$c_{r(\bar{bc})} = \frac{-r}{2}\begin{bmatrix} \frac{p_a+p_c-2p_b}{2p_a-p_c-p_b} & \frac{\sqrt{3}(p_a-p_c)}{2p_a-p_c-p_b} & 0 \end{bmatrix}^T \tag{21}$$

$$c_{r(\bar{ac})} = \frac{r}{2}\begin{bmatrix} 1 & \frac{\sqrt{3}(p_a-p_c)}{p_a+p_c-2p_b} & 0 \end{bmatrix}^T \tag{22}$$

Finally, the transformation matrix that rotates the gripper w.r.t. c_r is given in eq. (23) and eq. (24):

$$\text{Transf} = T(c_r) \cdot \text{Rot}(\hat{\omega}, \theta) \cdot T(-c_r) \tag{23}$$

$$\text{Transf} = \begin{bmatrix} I & c_r \\ 0 & 1 \end{bmatrix} \begin{bmatrix} \text{Rot}(\hat{\omega}, \theta) & 0 \\ 0 & 1 \end{bmatrix} \begin{bmatrix} I & -c_r \\ 0 & 1 \end{bmatrix} \tag{24}$$

TABLE I: Apple pick trials using the apple proxy and varying the branch stiffness and fruit localization error (offset)

Exp.	Stiffness	Offset [mm]	Reps	Time [s]
1	High	10	3	0.18 ± 0.03
2		20	3	4.59 ±0.60
3		30	3	9.36 ±1.07
4	Low	10	3	3.99 ±0.65
5		20	3	8.02 ±1.93
6		30	3	13.35 ±2.8

C. Experiments

We use a $UR5e$ manipulator with the multi-cup suction gripper as the EEF. Moreover, we use our apple proxy [2] to test our servoing protocol (fig. 3-*Right*). We vary the branch stiffness and the initial location of the gripper w.r.t. fruit to see their influence on the controller's performance. We measure the time elapsed between the first and last suction cup engagement as the performance metric. All experiments are summarized in table I.

1) Stiffness: Branch stiffness varies depending on the tree structure. Fruit trees in commercial orchards tend to have stiff branches due to pruning and trellis-based structures, whereas fruit trees in the wild can have long and less rigid branches. We hypothesize stiffer branches favor faster suction cup engagement, whereas loose branches hinder it. We tuned our proxy with low (210 N/m) and high (736 N/m) stiffness observed in previous research [1].

2) Fruit localization error: We mimick sensor localization inaccuracy by intentionally adding an offset to the pose of the EEF w.r.t. fruit center. We varied the offset from $10mm$, $20mm$, and $30mm$. This offset affects the number of suction cups that initially engage with the fruit and may affect the time required to engage the three suction cups.

III. Discussion

Foremost, in all trials summarized in table I the robot engaged the three suction cups and successfully picked the fruit from the proxy. As shown in fig. 3, during the servoing the air-pressure readings of the suction cups dropped below the vacuum threshold (i.e. $60kPa$), and then the gripper continued to pick the apple successfully. As expected, when the proxy was tuned with high stiffness, the robot engaged the three suction cups faster than when the proxy was tuned with low stiffness. This behavior is because the fruit dynamics show less resistance to swing away while the gripper pushes against it to engage all the suction cups. Similarly, when the offset increases, the robot takes longer to engage all the suction cups. This is due to the wider angular range that the robot sweeps to engage all the suction cups.

In future work, we will explore how the size of the fruit affects the performance of the controller. Additionally, we will investigate the maximum offset that the gripper can withstand while still successfully grasping and picking the fruit.

ACKNOWLEDGMENT

Funded in part by NSF grant 2024872 and USDA grant 2020-01461. The primary author thanks Fulbright-Colombia and Minciencias-Colombia for their financial support.

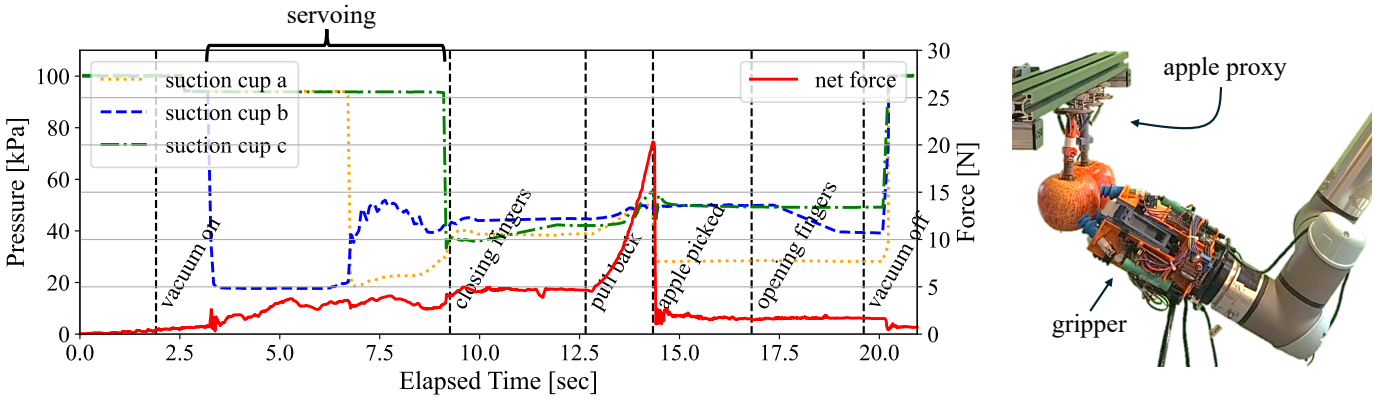

Fig. 3: Air pressure servoing for an apple pick using our apple proxy [2]. *Left*: Time series of air-pressure readings of each suction cup (left axis) and net force (right axis). The air pressure of suction cups b, a, and c drops below $60kPa$ when each suction cup engages with the fruit. In this case, the time between the engagement of the first (b) and the last suction cup (c) was $5.87s$. *Right:* Robotic manipulator with gripper using our apple proxy.

REFERENCES

[1] A. Velasquez, C. Grimm, and J. Davidson, "Dynamic evaluation of a suction based gripper for fruit picking using a physical twin," in *2024 IEEE International Conference on Robotics and Automation (ICRA)*, 2024, pp. 11 839–11 845.

[2] A. Velasquez, N. Swenson, M. Cravetz, C. Grimm, and J. R. Davidson, "Predicting fruit-pick success using a grasp classifier trained on a physical proxy," in *2022 IEEE/RSJ International Conference on Intelligent Robots and Systems (IROS)*, 2022, pp. 9225–9231.

[3] T. Li, F. Xie, Z. Zhao, H. Zhao, X. Guo, and Q. Feng, "A multi-arm robot system for efficient apple harvesting: Perception, task plan and control," *Computers and Electronics in Agriculture*, 2023.

[4] J.-e. Lee, R. Sun, A. Bylard, and L. Sentis, "Grasp Failure Constraints for Fast and Reliable Pick-and-Place Using Multi-Suction-Cup Grippers," Aug. 2024, arXiv:2408.03498 [cs]. [Online]. Available: http://arxiv.org/abs/2408.03498

[5] J. Lee, S. D. Lee, T. M. Huh, and H. S. Stuart, "Haptic Search With the Smart Suction Cup on Adversarial Objects," *IEEE Transactions on Robotics*, vol. 40, pp. 226–239, 2024. [Online]. Available: https://ieeexplore.ieee.org/document/10313081/

[6] K. M. Lynch and F. C. Park, *Modern Robotics: Mechanics, Planning, and Control*, 1st ed. Cambridge University Press, May 2017. [Online]. Available: https://www.cambridge.org/core/product/identifier/9781316661239/type/book